The Analyst

Speciation determination of arsenic in urine by high-performance liquid chromatography–hydride generation atomic absorption spectrometry with on-line ultraviolet photooxidation†

Dimiter L. Tsalev‡, Michael Sperling* and Bernhard Welz

Bodenseewerk Perkin-Elmer GmbH, Alte Nussdorfer Strasse, D-88662 Überlingen, Germany.
E-mail: Sperlimn@perkin-elmer.com

A coupled system for arsenic speciation determination based on high-performance liquid chromatography (HPLC), on-line UV photooxidation and continuous-flow hydride generation atomic absorption spectrometry (HGAAS) was built from commercially available modules with minor modifications to the electronic interface, the software and the gas–liquid separator. The best results were obtained with strong anion-exchange columns, Hamilton PRP X-100 and Supelcosil SAX 1, and gradient elution with phosphate buffers containing KH_2PO_4–K_2HPO_4. The on-line UV photooxidation with alkaline peroxodisulfate, 4% m/v $K_2S_2O_8$–1 mol l^{-1} NaOH, in a PTFE knotted reactor for 93 s ensures the transformation of inorganic As^{III}, monomethylarsonate, dimethylarsinate, arsenobetaine, arsenocholine, trimethylarsine oxide and tetramethylarsonium ion to arsenate. About 32–36 HPLC–UV–HGAAS runs could be performed within 8 h, with limits of detection between 2 and 6 µg l^{-1} As, depending on the species. The method was applied to the analysis of spot urine samples and certified urine reference materials (CRMs). Upon storage at 4 °C, reconstituted CRMs are stable for at least 2 weeks with respect to both their total arsenic content and the individual species distribution.

Keywords: *Arsenic speciation determination; high-performance liquid chromatography–hydride generation atomic absorption spectrometry; human urine; organoarsenic species; on-line ultraviolet photooxidation*

Many arsenic compounds are toxic and potentially carcinogenic, which raises much concern from environmental, occupational and nutritional points of view. However, the various inorganic and organic arsenic species exhibit large differences in their mobility, availability and toxicity in environmental and biological systems,[1] and can be approximately ranked in the following decreasing order of toxicity: As^{-III} (AsH_3) ≫ inorganic As^{III} (i-As^{III}, such as arsenite, metaarsenite and As_2O_3) > inorganic As^{V} (i-As^{V}, such as arsenate and metaarsenate) ≫ monomethylarsonate (MMA) > dimethylarsinate (DMA) ≫ 'fish arsenic' [such as arsenobetaine (AB), tetramethylarsonium ion (Me_4As^+) and arsenocholine (AC)]. Furthermore, these species can behave significantly differently during sampling, storage, sample preparation and generation of analytical signals.[2,3] It is therefore generally accepted that a species-selective determination of arsenic is needed for a meaningful risk assessment and better understanding of its biological and metabolic pathways and its analytical behavior. Speciation determination of arsenic has been addressed in more than 500 original publications and discussed in depth in several recent reviews[1,4–6] and book chapters.[2,3,7,8]

Human urine is a suitable biological specimen for monitoring recent exposure to arsenic because of its relatively fast excretion rates of this element from the organism. Misleading results, *i.e.*, an over-estimation of occupational exposure, may be obtained owing to the contribution of dietary arsenic of low toxicity (AB, DMA, Me_4As) when total arsenic is determined in urine, unless seafood is excluded from the diet for 3–5 days before sampling.[9–17] Several non-chromatographic procedures have been proposed to determine 'toxic arsenic' as a summation parameter. As the fish-derived organoarsenic species (AB, AC, Me_4As) do not form volatile hydrides, the sum of i-As^{III+V} and its organic metabolites (MMA and DMA) may be determined directly by HGAAS.[9–11,18] On-line wet oxidation of organoarsenic species, assisted by thermal[19–21] or microwave heating[13,22–30] or by UV irradiation,[18,22,31–40] is very attractive in view of automation of this non-chromatographic speciation analysis. Determining As with and without on-line oxidation gives a measure for the 'total As' and the 'toxic As'. On-line conversion of non-hydride forming organoarsenic species is indispensable in HPLC speciation techniques with post-column continuous-flow hydride generation (HG) such as HPLC–HGAAS,[19–21,29,30,36] HPLC–HG–ICP-OES,[8,32–34] or HPLC–HG–MIP-OES.[41] Interfacing HPLC with AAS *via* an on-line oxidation module and hydride generator does entail some sensitivity loss due to measuring the analyte as the less sensitive arsenate species and involves effects of several chemical and instrumental parameters on analytical performance that call for a thorough optimization and control of the entire analytical system. On-line pre-reduction of arsenate to the more sensitive i-As^{III} species[26,27,30,42] is not yet straightforward and entails dispersion problems and further complication of the chemical system. Nevertheless, for routine purposes the analysis of HPLC effluents by means of on-line UV photooxidation and continuous-flow HGAAS with a quartz tube atomizer (QTA) appears to be a more affordable instrumental approach than HPLC coupled with more expensive detectors such as ICP-MS[8,13–16,40,41,43–46] or electrospray ionization MS.[47]

The aim of this work was to design an automated system for flow injection (FI)–UV–HGAAS and HPLC-UV-HGAAS based on commercially available modules and to evaluate the role of instrumental and analytical parameters in the determination of some important arsenic species in urine.

Experimental

Instrumentation

A Perkin-Elmer Model 4100 atomic absorption spectrometer with an FIAS 400 flow injection system (mercury/hydride

† Presented at The Third International Symposium on Speciation of Elements in Toxicology and in Environmental and Biological Sciences, Port Douglas, Australia, September 15–19, 1997.

‡ On leave from the Faculty of Chemistry, University of Sofia, Sofia 1126, Bulgaria.

system mode), AS 91 autosampler, EDL II electrodeless discharge lamp and Epson LQ-870 printer, controlled by a Digital DECstation 425c computer with AA software Version 7.30 under GEM 3.11 and FIAS Firmware 6.1, was interfaced with a Model hwg 6808 beam boost photochemical reaction unit (ICT, International Chemie–Technik, Bad Homburg, Germany), as shown in Fig. 1(a). PTFE reaction coils (knotted reactors) of 0.5 mm id and lengths of 5, 10 and 15 m (Part Nos. IC89551, IC89552 and IC89553, respectively), providing irradiation times (t_{irr}) of 35, 70 and 105 s, respectively, with an 8 W UV lamp (254 nm) were used. In some experiments on the effect of heating on UV photooxidation[37] or on-line pre-reduction,[48] an extra 2 or 5 m knotted heating coil L_2, placed in a thermostated bath (TB) at 100 °C, was incorporated in the manifold for heating the liquid flow. Both peak-height (A_p) and integrated absorbance (A_{int}) measurements were used in FI–UV–HGAAS studies.

In the HPLC–UV–HGAAS mode [Fig. 1(b)], the mobile phase was delivered by means of a Perkin-Elmer Applied Biosystems (Foster City, CA, USA) Model 140 C Microgradient LC pump. The flow rates were varied between 0.7 and 1.4 ml min^{-1}. The thermostated bath and heating coil L_2 were omitted. The HPLC effluent was merged with an oxidant solution (Ox) and passed through a UV irradiation coil L_3. A Rheodyne (Cotati, CA, USA) Model 9725i syringe loading sample injector with a 50 μl sample injection loop made of polyetheretherketone (PEEK) (Upchurch Scientific, Oak Harbor, WA, USA) was used for sample injection. The integrated intensity for each measurement phase of the AA spectrometer was digitized using a 12 bit A/D converter synchronized to the instrument cycle using circuitry and software similar to that described by Lum *et al.*[49] installed in an Epson AXII PC. The absorbance was calculated for each cycle and applied to a 12 bit D/A converter after averaging. Thus a continuous analogue output of suitable range and time constant was generated for application to the output of a Perkin-Elmer Nelson (San Jose, CA, USA) Model 1022 integrator. Quantification was based on peak area measurements in the 'valley-to-valley' mode of baseline establishment. Optimized instrumental parameters are summarized in Table 1.

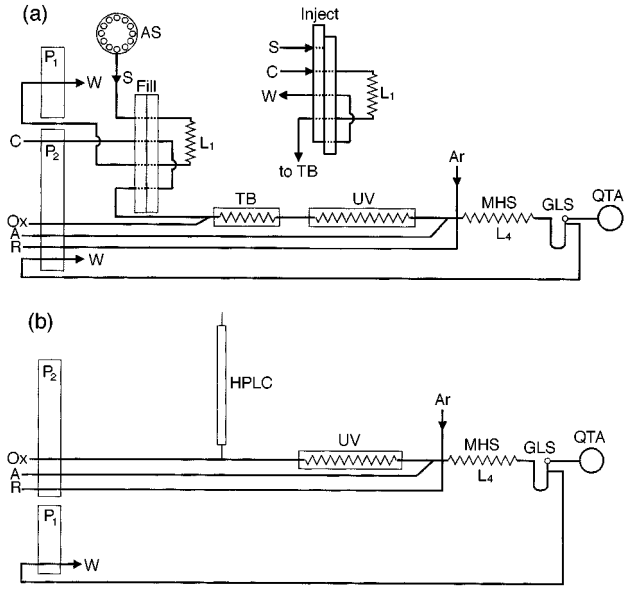

Fig. 1 Schematic diagram of the manifold and instrumental set-up for (a) FI–UV–HGAAS and (b) HPLC–UV–HGAAS. AS, autosampler; S, sample; C, carrier; P_1 and P_2, peristaltic pumps of the FIAS- 400 system; L_1, sample injection coil (in FIAS mode only); TB, thermostated bath with a heating coil L_2; UV, photochemical reaction unit with a PTFE irradiation coil L_3; MHS, mercury/ hydride system manifold with an MHS reaction coil L_4; Ox, oxidant; A, acid; R, reductant; W, waste; GLS, gas–liquid separator; QTA, quartz tube atomizer (for details see text and Table 1).

Reagents

Most solutions were prepared from analytical-reagent grade reagents (Merck, Darmstadt, Germany) unless stated otherwise. Stock standard solutions of inorganic and organic arsenic species containing 1000 μg ml^{-1} As were prepared from the reagents given in Table 2. Solutions of organoarsenic species at 1000 and 10 μg ml^{-1} As levels were stored in Teflon FEP flasks at 4 °C without adding any preservatives; more dilute working standard solutions were prepared fresh daily. Alkaline peroxodisulfate solutions containing 0.5–4% m/v $K_2S_2O_8$ and 0.5–2 mol l^{-1} NaOH were prepared daily. A stock standard solution of the reductant containing 6% m/v sodium tetrahydroborate ($NaBH_4$) (Riedel-de Haën, Seelze, Germany) and 1% m/v NaOH was stored in a refrigerator for up to 2 weeks and was diluted daily to yield 0.4–1% m/v $NaBH_4$ solutions containing NaOH and 0.08% v/v antifoaming agent (Dow Corning Antifoam 110 A Emulsion, Midland, MI, USA). Optimized concentrations and flow rates of reagents are given in Table 1.

Three HPLC columns with strong anion exchangers were evaluated: CompAx PEEK Spherisorb S SAX, 120 × 4 mm id, 5 μm film thickness, with a 15 mm pre-column (Knauer, Berlin, Germany); Supelcosil SAX 1, 250 × 4.6 mm id, 5 μm film thickness (with trimethylpropylamine groups) with a 20 mm pre-column (Sigma–Aldrich Chemie, Geschäftsbereich Supelco, Deisenhofen, Germany); and Hamilton PRP X-100, 250 × 4 mm id, 10 μm film thickness [with poly(styrene–divinylbenzene) with trimethylammonium exchanger] with a 20 mm pre-column (CS Chromatographie Service, Langerwehre, Germany).

To prepare the mobile phases, phosphate buffers with pH values between 2.22 and 8.48, containing 5–30 mmol l^{-1}

Table 1 Optimized instrumental and analytical parameters for FI–UV–HGAAS and HPLC–UV–HGAAS

Parameter	Setting
Lamp power	EDL II, 350 mA
Wavelength	193.7 nm
Bandpass	2 nm (low)
Deuterium background correction	AA–BG mode
Quartz cell temperature	900 °C
Gas–liquid separator	Type B (Fig. 4), fed and drained *via* PTFE capillaries (see text)
Integration time (FIAS mode)	49 s
Sample injection coil	100 μl (PTFE, L_1, FIAS mode) 50 μl (PEEK, HPLC mode)
UV irradiation coil (L_3)	PTFE knotted reactor, 10 m × 0.5 mm id
MHS reaction coil (L_4)	PTFE knotted reactor, 1 m × 0.8 mm id
Flow rate of oxidant (Ox), acid (A) and reductant (R)	0.5 ml min^{-1} at 70 rev min^{-1} of pump 2 with 'green/yellow' tubing, 0.44 mm id
Flow rate of mobile phase	1 ml min^{-1}
Flow rate of Ar purge gas	45 ml min^{-1}
Drainage of GLS	100 rev min^{-1} of pump 1 with 'red/red' tubing, 1.14 mm id
Oxidant (Ox)	4% m/v $K_2S_2O_8$–1 mol l^{-1} NaOH
Acid (A)	4 mol l^{-1} HCl
Reductant (R)	1% m/v $NaBH_4$–0.17% m/v NaOH–0.08% v/v antifoaming agent
Mobile phase	Phosphate buffers (see text for optimum compositions with different HPLC columns)

PO_4^{3-}, were prepared fresh daily from orthophosphoric acid (H_3PO_4), potassium dihydrogenphosphate (KH_2PO_4) and anhydrous dipotassium hydrogenphosphate (K_2HPO_4) and were filtered through a 0.45 μm PTFE membrane, purged and pressurized with helium (99.995% v/v) (Linde, Unterschleissheim, Germany).

Urine samples and Certified Reference Materials

The Standard Reference Material SRM 2670 Toxic Metals in Freeze-Dried Urine (Normal and Elevated Level) from the National Institute of Standards and Technology (NIST) (Gaithersburg, MD, USA) and Lyphochek Urine Metals Control Level 1, Lot No. 69021, and Level 2, Lot No. 69022, from Bio-Rad Laboratories (Munich, Germany) were reconstituted with de-ionized water as recommended by the manufacturers. Samples denoted 'fish-eater's urine' were 'spot' samples of first morning urine obtained 10 h after consumption of 100 g of shrimps and 100 g of tuna fish. Urine samples and CRMs were filtered through a 0.45 μm membrane, FP 030/20 White Rim disposable filter holder (Schleicher and Schuell, Dassel, Germany) before analysis and analyzed the same day except when stability on storage at 4 °C was being studied.

Results and discussion

A number of instrumental and analytical parameters require optimization in speciation analysis by HPLC–HGAAS. The effects of some variables are illustrated in Figs. 2–4 and Table 3, and the recommended optimum conditions are summarized in Table 1. Among the most important considerations are matching of the flow rates (F_l) of fluids in the entire analytical system, ensuring high and reproducible responses from all inorganic and organic arsenic species, achieving baseline HPLC separation within a reasonable time and providing high signal-to-noise ratios, *i.e.*, good limits of detection (LOD).

Flow rates of carrier or HPLC mobile phase

Typical flow rates of the mobile phase for HPLC columns of 4.0–4.6 mm id are between 0.5 and 1.5 ml min^{-1}, which are significantly lower than the optimum flow rates of the carrier in FI–HGAAS systems, *viz.*, 4–7 ml min^{-1}. Decreasing the flow rate of the carrier to 1 or 0.5 ml min^{-1} [Fig. 2(a)] and correspondingly also of other reagents resulted in more pronounced signal fluctuations and dispersion due to pulsation of peristaltic pumps at low pump speeds and higher noise levels produced during gas–liquid separation in the MHS reaction coil (L_4) and gas–liquid separator (GLS).

The flow rate of the carrier was fixed at 1 ml min^{-1} in FI–HGAAS and FI–UV–HGAAS experiments, and efforts were made to decrease signal fluctuations by optimizing other parameters, such as addition of an antifoaming agent, construction of GLS, Ar flow rate and length of L_4. The dual-syringe solvent delivery system was found to produce much less fluctuation in HPLC–UV–HPLC measurements than the peristaltic pump in FI–UV–HGAAS experiments.

Effect of antifoaming agent

Preliminary experiments with the addition of an antifoaming agent to the reductant solution showed that gas–liquid separation was smoother and signal fluctuations were reduced by about fivefold [Fig. 2(b)]. This was in agreement with previous experience with direct FI–HGAAS[18] and FI–on-line microwave-assisted digestion–HGAAS[23,24] in the analyses of urine samples. Hence the concentration of antifoaming agent in the $NaBH_4$ solution was kept at an optimal level of 0.08% v/v in all further experiments; increasing its concentration above 0.1% v/v entailed a decrease in sensitivity.

UV Photooxidation

Optimization of UV photooxidation of organoarsenic and organotin species with alkaline and acidic peroxodisulfate, respectively, in an FI–UV–HGAAS system has been discussed in more detail elsewhere.[37] The concentrations of $K_2S_2O_8$ and NaOH are not critical within the ranges 0.5–4% m/v and 0.4–2 mol l^{-1}, respectively, and recoveries of i-As^{III}, i-As^{V}, MMA, DMA, AB and AC were between 91 and 101% with a 10 m reactor (irradiation time t_{irr} = 70 s). Additional experiments performed with two other non-hydride forming species, TMAO and Me_4As, resulted in recoveries of 114 ± 4 and 102 ± 5% with 1% m/v $K_2S_2O_8$–0.5 mol l^{-1} NaOH and 103 ± 3 and 94 ± 9% with 4% m/v $K_2S_2O_8$–0.5 mol l^{-1} NaOH, respectively.

In HPLC–UV–HGAAS measurements, the concentrations of peroxodisulfate and NaOH in the oxidant solution were kept at their maximum levels, 4% m/v $K_2S_2O_8$–1 mol l^{-1} NaOH, while the flow rate of the oxidant was decreased from 1 to 0.5 ml min^{-1}, providing longer irradiation/reaction times (93 *versus* 70 s) in the knotted reactor (10 m × 0.5 mm id) without causing any apparent peak broadening. The thermostated bath (TB) with a heating coil L_2 was omitted since it had only a minor effect on UV photooxidation of organoarsenicals but entailed a shortened lifetime of the quartz lamp wrapped with a heated coil. The overall effect of the UV photochemical reaction unit was an apparent increase in the HPLC retention times by about 2 min (consisting of t_{irr} = 93 s + travel times in T-pieces and connections). However, UV photooxidation resulted not only in the transformation of all analyte species into a definite chemical form, i-As^{V}, but also in a substantial decrease in sensitivity (2–7 -fold) because hydride generation is significantly slower from i-As^{V} than i-As^{III}. Therefore, the HG conditions require careful optimization.

Table 2 Arsenic species

Abbreviation	Formula	Compound and solvent	Supplier*
i-As^{III}	$NaAsO_2$	As_2O_3 in NaOH solution	A
i-As^{V}	H_3AsO_4	Arsonic acid in 0.5 M HCl	B
MMA	$CH_3AsO_3Na_2 \cdot 6H_2O$	Sodium methylarsonate	C
DMA	$(CH_3)AsO_2Na \cdot 3H_2O$	Dimethylarsinic acid, sodium salt	D
AB	$(CH_3)_3As^+CH_2COO^-$	Arsenobetaine in water	D
AC	$(CH_3)_3As^+CH_2CH_2OHBr$	Arsenocholine bromide in water	D
TMAO	$(CH_3)_3AsO$	Trimethylarsine oxide in water	E
Me_4As	$(CH_3)_4AsI$	Tetramethylarsonium iodide in water	E

* A, Riedel-de Haën, Seelze, Germany; B, Merck, Darmstadt, Germany; C, Carlo Erba, Milan, Italy; D, Community Bureau of Reference (BCR), Brussels, Belgium; and E, donated by Dr. Walter Goessler, University of Graz, Austria.

Length of the reaction coil L_4 in the MHS manifold

Hydride generation and stripping from solutions in flow systems is strongly kinetically controlled, increased reaction times on increasing the length of the coil L_4 therefore had a marked effect on the i-As^{III} signal [Fig. 2(c)]. The integrated absorbance doubled with a knotted reactor (KR, 100 cm × 0.8 mm id) *versus* a minimum length (RC, 10 cm × 0.5 mm id) of PTFE tubing. The integrated absorbance of the i-As^{V} species was increased sevenfold under the same conditions. Hence the loss of sensitivity caused by HPLC–UV–HGAAS measurements of i-As^{V} can be substantially alleviated by employing a long reaction coil L_4. Unfortunately, using longer reaction coils also entails more pronounced signal fluctuations [see Fig. 2(c)].

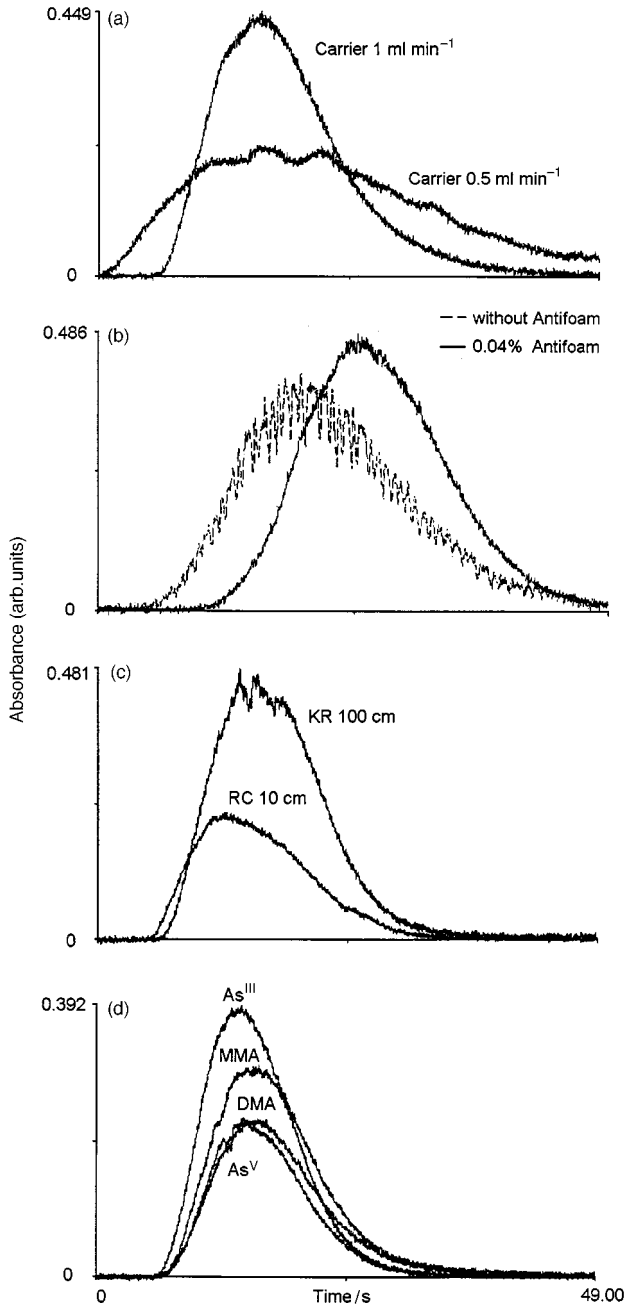

Fig. 2 Typical flow injection peaks illustrating optimization of hydride generation module at 10 ng As levels. (a) Effect of low flow rate of carrier; (b) effect of antifoam addition; (c) effect of the length of MHS reaction coil L_4, a 100 cm knotted reactor (KR), *versus* a straight 10 cm reaction coil (RC); (d) signals for four hydride-forming arsenic species under optimized conditions (0.5 mol l^{-1} HCl, 1% m/v $NaBH_4$, 100 cm KR).

Concentrations and flow rates of reagents

A 1% m/v $NaBH_4$ solution, which is a higher concentration than usual, was found to result in a better sensitivity for the i-As^{V} species and a better signal-to-noise ratio [Fig. 2(d)]. The effect of HCl concentration in the acidification channel on the integrated absorbance signals for i-As^{III}, i-As^{V}, MMA and DMA species in FI– HGAAS is shown in Fig. 3. The sensitivity for i-As^{V} increases with increasing acid concentration, and a concentration of 4 mol l^{-1} was found to be the optimum after UV photooxidation, whereas a 0.5 mol l^{-1} HCl concentration provided good compromise conditions for measuring the other hydride forming species, i-As^{III}, MMA and DMA [Fig. 2(d)]. Under these conditions, TMAO gives a very small response of about 10% of that for i-As^{III}, whereas AB, AC and Me_4As produce no hydride at all.

The flow rate of the Ar purge gas affects the sensitivity and the signal stability in opposite ways. The lower the gas flow rate, the better is the sensitivity, because of the dilution effect of the purge gas. At the same time, however, signal fluctuations are more pronounced at low Ar flow rates; hence a compromise flow rate of 45 ml min^{-1} was employed in all measurements. Using higher flow rates of 50, 60 and 70 ml min^{-1} entailed decreases in sensitivity by 3, 23 and 32%, respectively, for i-As^{III} in integrated absorbance.

Construction of the gas–liquid separator

Four GLSs, which are shown schematically in Fig. 4, were evaluated, aiming at improved signal-to-noise ratios, sensitivities for i-As^{V} and other performance characteristics given in Table 3. The mode of feeding and draining of the GLS was found to be particularly important. The gas–liquid flow emerging from the outlet of the capillary L_4 forms a jet about 7–8 cm long which can be a source of excessive noise when it

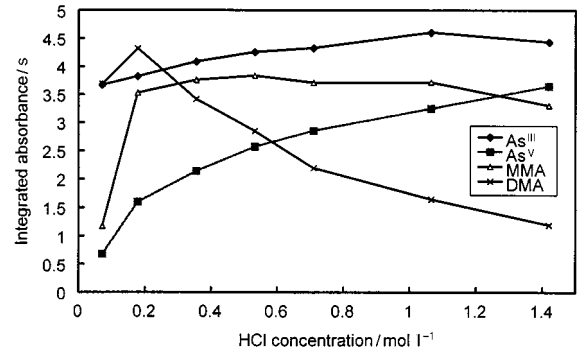

Fig. 3 Effect of HCl concentration in the acidification channel on the integrated absorbance signal for four arsenic species (2.5 ng As each) in HPLC–HGAAS mode.

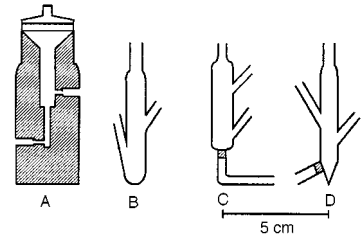

Fig. 4 Schematic depiction of four different designs of gas–liquid separators and typical peak shapes for 5 ng of i-As^{III} obtained with these separators in FI–HGAAS.

is not directed in a proper manner within the GLS. More aerosol and pulsation are produced when the jet feeds the upper part of the GLS; better results are obtained when it impacts the wall close to the bottom of the GLS. The worst performance was obtained with the GLSs with a frit at the bottom (type C) or at the side (type D), in which the formation of even a small layer of liquid on the bottom because of 'underdraining' the GLS resulted in bubbling and excessive noise. Better results were obtained when the GLSs types B, C and D were fed and drained by means of PTFE capillaries (0.8 mm id) fitted into the side-arms of these GLSs, whereby the outlet (drain) capillary touched the lowest bottom part of the GLS while the inlet capillary was about 2 mm away from the drain capillary in GLS type B or C or touched the upper part of the side frit of the GLS type D. Smooth draining was facilitated by always using higher flow rates in the drain channel by means of an independently controlled pump 1, *i.e.*, the GLS was working in an 'over-draining' mode. This arrangement minimized flooding, bubbling and aerosol formation; however, it also affected the sensitivity slightly, as part of the gaseous phase is also pumped to waste. As can be seen from the results in Table 3, GLS type B showed the best overall performance and was adopted in subsequent HPLC–UV–HGAAS work.

HPLC separation conditions

The composition, concentration and pH of the phosphate buffers (mobile phase) were optimized for three HPLC columns with strong anion exchangers. With a Spherisorb S SAX column and 10 mmol l^{-1} KH_2PO_4–K_2HPO_4 at pH 7.5–7.8, the retention times for DMA, i-As^{III}, MMA and i-As^{V} were 2.17, 2.25, 3.30 and 5.80 min, respectively; the first two peaks of DMA and i-As^{III} could not be separated. With a Supelcosil SAX 1 column and a mobile phase of 20 mmol l^{-1} KH_2PO_4 at pH 4.64, the retention times for AC + Me_4As, i-As^{III}, AB, DMA + TMAO, MMA and i-As^{V} were 5.0, 6.0, 6.6, 7.8, 14.5 and 15.6 min, respectively. Again, some species could not be resolved. Increasing the pH of the mobile phase (KH_2PO_4–K_2HPO_4, 20 mmol l^{-1} PO_4^{3-}) to 6.2–7.3 resulted in faster elution of the MMA (9.5 min) and i-As^{V} (10.2 min) but impaired the separation of the early eluting species: i-As^{III} (6.2 min), AB (6.2 min) and AC (6.2 min). Typical chromatograms with and without UV photooxidation are shown in Fig. 5. Applications to urine samples are demonstrated in Fig. 6: chromatogram A (from a person with occupational exposure) shows peaks for 39 μg l^{-1} of i-As^{III} and 15 μg l^{-1} of As as DMA species; chromatogram B (a fish-eater's urine) shows peaks for AB, DMA and i-As^{V} (300, 19 and 10 μg l^{-1} As, respectively).

Similar results but improved resolution of MMA and i-As^{V} species were obtained with a Hamilton PRP X-100 column and gradient elution with KH_2PO_4–K_2HPO_4 buffer (pH 6.22) as shown in Fig. 7. Chromatographic separation started with 12

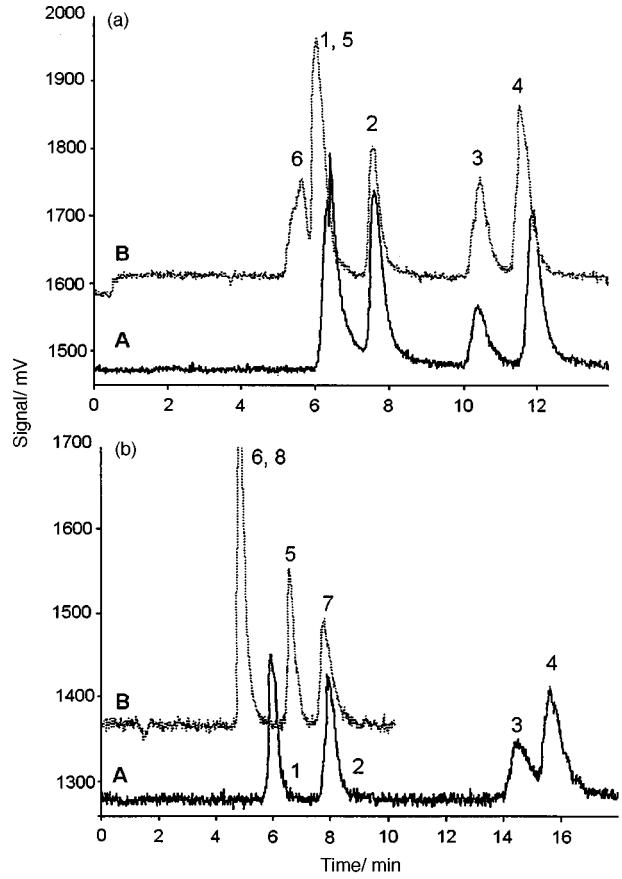

Fig. 5 Chromatograms from anion-exchange HPLC–UV–HGAAS of arsenic species (2.5 ng of As each) in standard solutions with a Supelcosil SAX1 column, (a) without and (b) with oxidant addition and UV irradiation. Peaks: 1, i-As^{III}; 2, DMA; 3, MMA; 4, i-As^{V}; 5, AB; 6, AC; 7, TMAO; and 8, Me_4As. Mobile phase: 20 mmol l^{-1} phosphate buffer (KH_2PO_4–K_2HPO_4), (a) pH 6.85 and (b) pH 4.64, at a flow rate of 1 ml min^{-1}.

Table 3 Comparison of four gas–liquid separators (GLS) for FI–HGAAS at carrier flow rates of 1 ml min^{-1}. For design details see Fig. 4

Parameter	Type A	Type B	Type C	Type D
Total internal volume of GLS/μl	2150	4500	1200	2100
Construction material of GLS	PMP*	BSG†	BSG†	BSG†
Other characteristics of GLS	PTFE membrane‡	—	Bottom frit§	Side frit§
Characteristic mass m_o for A_{int}	7.4	6.7	6.5	3.9
Characteristic mass m_o for A_p	114	123	105	108
RSD (%) (A_{int})¶	3.8	2.6	1.7	7.3
RSD (%) (A_p)¶	3.4	1.5	6.2	2.9
i-As^{III}/i-As^{V} sensitivity ratio (Q_A)	2.8	2.3	2.4	3.0
i-As^{III}/i-As^{V} sensitivity ratio (A_p)	2.8	2.4	2.5	2.8
Compatibility with organic solvents‖	−−−	+++	N.e.††	N.e.
Compatibility with heating**	+	+++	−	−−
Signal stability	++	+++	−−	−−−
Stability against flooding	+	+++	−−−	−−
Washout (signal to baseline)	+++	++	++	−−

* Polymethylpentene. † Borosilicate glass. ‡ PTFE membrane (Part No. B050-8567) on top of GLS. § Robu-Glass filter, diameter 5 mm, porosity P 1.6, No. 5 (Robuglasfilter-Geräte, Hattert, Germany). ¶ n = 5–6 at the 5 ng i-As^{III} level. ‖ Tested with a methanol– acetonitrile–water (40 + 30 + 30, v/v) mobile phase. ** Thermostated bath at 100 °C. †† N.e., not evaluated.

mmol l^{-1} phosphate buffer and continued after 6 min with a 'stronger' eluent, 24 mmol l^{-1} PO_4^{3-}, in order to decrease the retention time for the strongly retained species, i-As^{V}, from 14.4 to 11.7 min. The system showed good long-term stability with retention times of 4.43 ± 0.02, 5.51 ± 0.08, 6.69 ± 0.24 and 11.70 ± 0.06 min (RSD 0.5–3.6%) for i-As^{III}, DMA, MMA and i-As^{V}, respectively, during 10 successive chromatographic runs over 2 h. Arsenobetaine, the most common fish-derived organoarsenic species, is eluted together with i-As^{III} but could be determined by difference from two chromatographic runs: with (AB + i-As^{III}) and without UV photooxidation (i-As^{III} only) as shown in Fig. 7. The limit of detection in urine samples expressed as three times the standard deviation for arsenic in a blank solution was 0.2 ng or 4 μg l^{-1} As with UV photooxidation and 2, 4, 3 and 6 μg l^{-1} As without UV photooxidation for i-As^{III}, i-As^{V}, MMA and DMA, respectively.

Analysis of urine CRMs

Four samples of freeze-dried urine CRMs were analyzed by HPLC–UV–HGAAS with a Hamilton PRP X-100 column: the NIST SRM 2670 Normal and Elevated Levels on the days 1, 7 and 14 after reconstitution and the Bio-Rad Lyphochek Urine Metals Control Levels 1 and 2 on days 1 and 9 after reconstitution. Samples were stored at 4 °C between analyses. No significant difference in arsenic speciation was found during storage, which is in agreement with some recent reports (Ritsema and van Heerde[38] found the total arsenic in urine to be

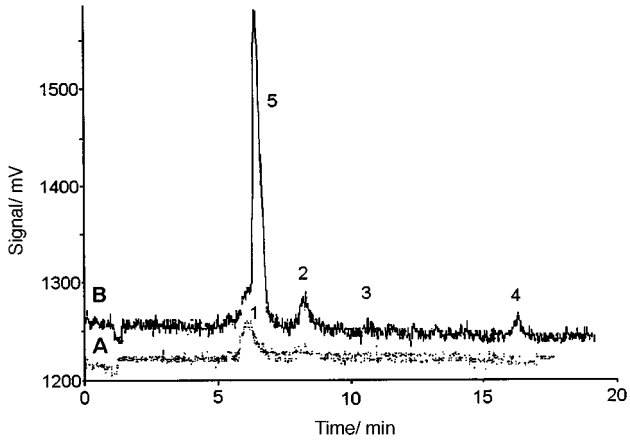

Fig. 6 Chromatograms from anion-exchange HPLC–UV–HGAAS of arsenic species in 50 μl urine samples with a Supelcosil SAX1 column with oxidant addition and UV irradiation. Peaks as in Fig. 5. A, urine sample from an occupationally exposed person; and B, B urine sample from a fish eater.

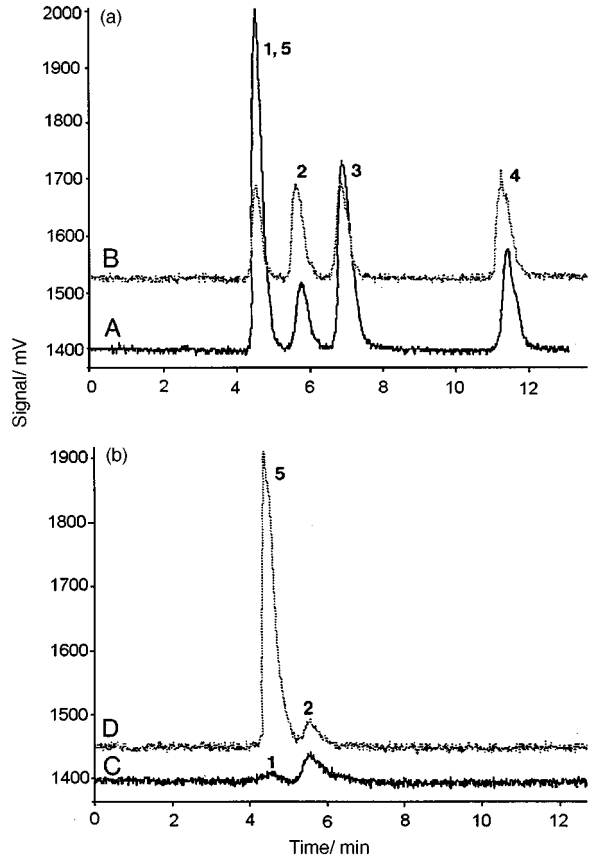

Fig. 7 Chromatograms from anion-exchange HPLC–UV–HGAAS of arsenic species with a Hamilton PRP X-100 column and gradient elution with KH_2PO_4–K_2HPO_4 buffer, pH 6.22 (0–6 min, 12 mmol l^{-1} PO_4^{3-}; 6–13 min, 24 mmol l^{-1} PO_4^{3-}). Peaks as in Fig. 5. Chromatograms A and C without and chromatograms B and D with oxidant addition and UV irradiation; A and B, standard solutions containing 2.5 ng of As each; C and D, urine sample (fish-eater's urine).

Table 4 Arsenic speciation determination by HPLC–UV–HGAAS in NIST SRM 2670 Toxic Metals in Freeze-Dried Urine Normal and Elevated Levels (in μg l^{-1} As). Means ± SD from three series of measurements with three parallels in each series on days 1, 5 and 14 after reconstitution with intermediate storage at 4 °C

Urine sample	Certified value and confidence limits	i-As^{III}	i-As^{V}	MMA	DMA	AB	Sum of all species determined
Normal Level, this work (−/−)*	60‡	< 2	< 4	12.8 ± 2.0	52.4 ± 7.6	N.d.§	65.2
Normal Level, this work (−/−)†		< 4	< 4	18.4 ± 4.4	48.3 ± 2.8	35.6 ± 7.8	102.3
Normal Level, ref. 46		N.d.	N.d.	N.d.	N.d.	N.d.	62.8 (58–66) (i-As + MMA + DMA)
Normal Level, ref. 43		52.6 ± 4.1	0.8 ± 0.5	9.9 ± 1.4	45.5 ± 3.5	N.d.	109 ± 6
Elevated Level, this work (−/−)*	480 ± 100	< 2	417 ± 64	12.9 ± 4.2	52.3 ± 10.2	N.d.	482.2
Elevated Level, this work (−/−)†		< 4	416 ± 40	15.9 ± 3.8	48.9 ± 2.0	32.0 ± 8.4	513
Elevated Level, ref. 43		43.8 ± 9.1	406 ± 153	5.0 ± 3.6	34.8 ± 8.7	N.d.	489 ± 154
Elevated Level, collaborative study, ref. 50		N.d.	N.d.	15.5 ± 4.3	52.2 ± 4.3	(~30)	430 ± 56 (total i-As^{III+V}) 487 ± 54 (i-As + MMA DMA) 502 ± 50 (total As)

* No UV photolysis/no oxidant. † With UV photolysis and oxidant. ‡ Information value only. § N.d., not determined.

Table 5 Arsenic speciation determination by HPLC–UV–HGAAS in Bio-Rad Lyphochek Urine Metals Control Levels 1 and 2 (in μg l^{-1} As, n = 4–6)

Urine sample	Certified value and confidence limits	i-As^{III}	i-As^{V}	MMA	DMA	AB	Sum of all species determined
Level 1 (−/−)*	52 (42–62)	< 2	55 ± 11	< 3	10 ± 2	N.d.‡	65
Level 1 (+/+)†		< 4	58 ± 4	< 4	15 ± 6	26 ± 11	99
Level 2 (−/−)*	152 (121–182)	< 2	145 ± 21	< 3	35 ± 14	N.d.	180
Level 2 (+/+)†		< 4	151 ± 21	< 4	13 ± 4	30 ± 11	194

* No UV photolysis/no oxidant. † With UV photolysis and oxidant. ‡ N.d., not determined.

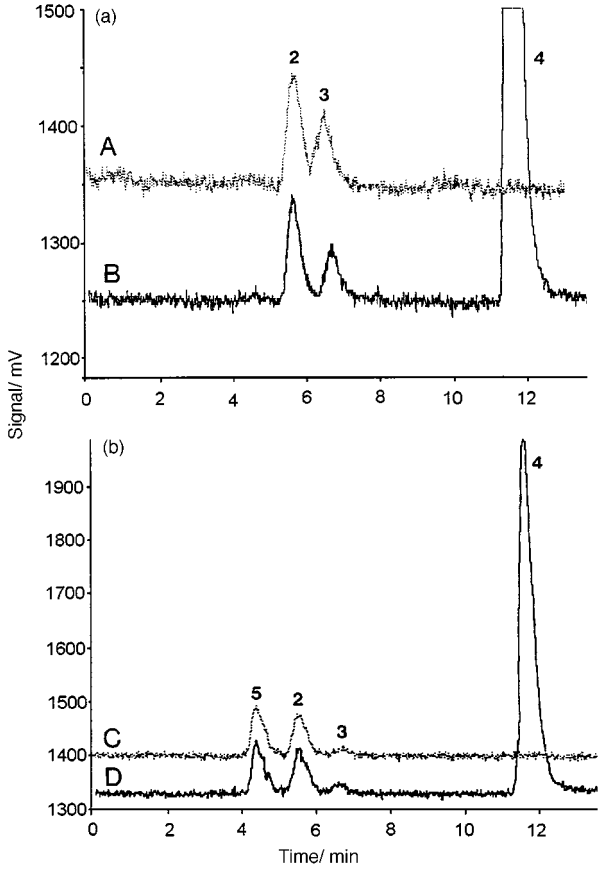

Fig. 8 Arsenic speciation in NIST SRM 2670 Toxic Metals in Freeze-Dried Urine. A and C, Normal Level; B and D, Elevated Level; A and B, without oxidant addition and UV irradiation; C and D, with oxidant and UV irradiation. Chromatographic conditions as in Fig. 7.

stable during storage for 30 d at 5 ± 4 °C, Crecelius and Yager[50] found their intercomparison samples to be relatively stable during storage and shipping and Mürer *et al.*[11] found arsenobetaine and arsenocholine to be relatively stable during storage in the dark during 21 d but observed some loss in daylight). The mean values of all determinations are presented in Tables 4 and 5. Typical chromatograms for both levels of NIST SRM 2670 samples are shown in Fig. 8 and reveal that the Normal and Elevated Levels are identical in their matrix and contents of the arsenic species except that the Elevated Level is spiked with about 410 μg l^{-1} of i-As^{V}. Another finding was that all four reference materials contain AB, the contribution of which to the total content may have been underestimated during the analytical certification. Some probable reasons for such an underestimation could be the use of quantification procedures based on direct HG or solvent extraction without complete mineralization of the non-reactive AB or DMA, which gives a lower response in direct HGAAS. At least two recently published studies reported the presence of AB in NIST SRM 2670. Pergantis *et al.*[47] found 11 ± 3 μg l^{-1} of AB (as As) by microbore HPLC coupled on-line with electrospray ionization mass spectrometry. Another laboratory reported approximately 30 μg l^{-1} of AB (as As) by HPLC–ICP-MS in a recent intercomparison speciation study.[50] Several recent publications reported higher total contents than the information value for As in NIST SRM 2670 Normal Level, such as 69,[51] 81 ± 1[52] and 109 ± 6 μg l^{-1}[43] by ICP-MS, 84 ± 2 μg l^{-1} by FI–HGAAS after UV photolysis[22] and 80 ± 6 μg l^{-1} by direct ETAAS[22] *versus* 62 ± 2 μg l^{-1} by FI–HGAAS without UV photolysis.[22] Accordingly, higher mean values were also published for the Elevated Level material, such as 489 ± 154[43] and 491 ± 3 μg l^{-1}[52] by ICP-MS, 545 ± 4 μg l^{-1} by FI–HGAAS after off-line UV photolysis[38] and 530 ± 42 and 540 ± 19 μg l^{-1} by FI–HGAAS after off-line digestion followed by two different on-line pre-reduction FI–HGAAS procedures.[20] The results of our study as presented in Table 4 are generally in good agreement with the recent interlaboratory exercise on arsenic speciation in urine, reported by Crecelius and Yager.[50] However, we were unable to find any i-As^{III} in these samples, as previously reported by Heitkemper *et al.*[43] using HPLC–ICP-MS (see Table 4). One possible explanation for this discrepancy could be that the i-As^{III} and AB were not resolved in the HPLC separation by Heitkemper *et al.*[43] and the peak for AB was attributed to i-As^{III}. More work is obviously required before these coupled techniques reach maturity and can enter routine toxicological laboratories.

Conclusions

The coupling of anion-exchange HPLC and continuous-flow HGAAS, with and without on-line UV photooxidation by alkaline peroxodisulfate, is a suitable and affordable approach to the speciation determination of toxicologically important arsenic species in urine. Although the characteristic mass (m_0 = 0.01 ng) and absolute LODs (0.1–0.3 ng) were very low, the relative LODs were impaired to 2–6 μg l^{-1} because of the small sample volumes (50 μl) and because hydride generation was from the oxidized, less sensitive i-As^{V} species. Some instrumental and chemical parameters that affected analytical performance were identified and optimized. Speciation analysis of urine CRMs revealed the presence of significant amounts of arsenobetaine in these materials, resulting in higher total arsenic levels than previously recommended or certified.

The authors are grateful to J. Bauslaugh and B. Radziuk for the modification of the software and interface between the AA spectrometer and the PE Nelson integrator and to W. Goessler for providing standard solutions of TMAO and Me_4As.

References

1 Cullen, W. R., and Reimer, K. J., *Chem. Rev.*, 1989, **89**, 713.
2 Tsalev, D. L., *Atomic Absorption Spectrometry in Occupational and Environmental Health Practice, Vol. III: Progress in Analytical Methodology*, CRC Press, Boca Raton, FL, 1995, ch. 3, pp. 19–31.

3 Dedina, J., and Tsalev, D. L., *Hydride Generation Atomic Absorption Spectrometry*, Wiley, Chichester, 1995, ch. 8, pp. 182–245.
4 Morita, M., and Edmonds, J. S., *Pure Appl. Chem.*, 1992, **64**, 575.
5 González Soto, E., Alonso Rodriguez, E., Fernández Fernández, E., and Prada Rodriguez, D., *Ciencia*, 1996, **4**, 149.
6 Burguera, M., and Burguera, J. L., *Talanta*, 1997, **44**, 1581.
7 Irgolic, K. J., in *Hazardous Metals in the Environment*, ed. Stoeppler, M., Elsevier, Amsterdam, 1992, pp. 287–350.
8 Caroli, S., La Torre, F., Petrucci, F., and Violante, N., in *Element Speciation in Bioinorganic Chemistry*, ed. Caroli, S., Wiley, New York, 1996, ch. 13, pp. 445–463.
9 Foà, V., Colombi, A., Maroni, M., Buratti, M., and Calzaferri, G., *Sci. Total Environ.*, 1984, **34**, 241.
10 Chana, B. S., and Smith, N. J., *Anal. Chim. Acta*, 1987, **197**, 177.
11 Mürer, A. J. L., Abildtrup, A., Poulsen, O. M., and Christensen, J. M., *Analyst*, 1992, **117**, 677.
12 SAS Trace Element Laboratories, *Clinical and Analytical Handbook*, ed. Walker, A. W., Royal Surrey County and St. Luke′s Hospitals, Guildford, 2nd edn., 1992.
13 Le, X.-C., Cullen, W. R., and Reimer, K. J., *Talanta*, 1993, **40**, 185.
14 Shibata, Y., and Morita, M., *Anal. Sci.*, 1989, **5**, 107.
15 Goessler, W., Schlagenhaufen, C., Kuehnelt, D., Greschonig, H., and Irgolic, K. J., *Appl. Organomet. Chem.*, 1997, **11**, 327.
16 Le, X.-C., Cullen, W. R., and Reimer, K. J., *Clin. Chem.*, 1994, **40**, 617.
17 Le, X. C., Ma, M., and Wong, N. A., *Anal. Chem.*, 1996, **68**, 451.
18 Guo, T., Baasner, J., and Tsalev, D. L., *Anal. Chim. Acta*, 1997, **349**, 313.
19 López, M. A., Gómez, M. M., Palacios, M. A., and Cámara, C., *Fresenius' J. Anal. Chem.*, 1993, **346**, 643.
20 Stummeyer, J., Harazim, B., and Wippermann, *Fresenius' J. Anal. Chem.*, 1996, **354**, 344.
21 Palacios, M. A., Gómez, M., Cámara, C., and López, M. A., *Anal. Chim. Acta*, 1997, **340**, 209.
22 Willie, S. N., *Spectrochim. Acta, Part B*, 1996, **51**, 1781.
23 Tsalev, D. L., Sperling, M., and Welz, B., *Analyst*, 1992, **117**, 1729.
24 Tsalev, D. L., Sperling, M., and Welz, B., *Analyst*, 1992, **117**, 1735.
25 Le, X.-C., Cullen, W. R., and Reimer, K. J., *Appl. Organomet. Chem.*, 1992, **6**, 161.
26 Welz, B., He, Y., and Sperling, M., *Talanta*, 1993, **40**, 1917.
27 Sperling, M., He, Y., and Welz, B., in *CANAS'93 Colloquium Analytische Atomspektroskopie*, ed. Dittrich, K., and Welz, B., Universitat Leipzig und UFZ-Umweltforschungszentrum Leipzig-Halle, Leipzig, 1993, pp. 989–1004.
28 Le, X.-C., Cullen, W. R., and Reimer, K. J., *Talanta*, 1994, **41**, 495.
29 López-Gonzálvez, M. A., Gómez, M. M., Cámara, C., and Palacios, M. A., *J. Anal. At. Spectrom.*, 1994, **9**, 291.
30 Lamble, K. J., and Hill, S. J., *Anal. Chim. Acta*, 1996, **334**, 261.
31 Atallah, R. H., and Kalman, D. A., *Talanta*, 1991, **38**, 167.
32 Rubio, R., Peralta, I., Alberti, J., and Rauret, G., *J. Liq. Chromatogr.*, 1993, **16**, 3531.
33 Rubio, R., Alberti, J., and Rauret, G., *Int. J. Environ. Anal. Chem.*, 1993, **52**, 203.
34 Rubio, R., Padró, A., Alberti, J., and Rauret, G., *Anal. Chim. Acta*, 1993, **283**, 160.
35 Rubio, R., Alberti, J., Padro, A., and Rauret, G., *Trends Anal. Chem.*, 1995, **14**, 274.
36 Howard, A. G., and Hunt, L. E., *Anal. Chem.*, 1993, **65**, 2995.
37 Tsalev, D. L., Sperling, M., and Welz, B., in, *CANAS'97 Colloquium Analytische Atomspektroskopie*, ed. Werner, G., Universitat Leipzig und UFZ-Umweltforschungszentrum Leipzig–Halle, Leipzig, in the press.
38 Ritsema, R., and van Heerde, E., *Fresenius' J. Anal. Chem.*, 1997, **358**, 838.
39 Zhang, X., Cornelis, R., De Kimpe, J. and Mees, L., *Anal. Chim. Acta*, 1996, **319,** 177.
40 Zhang, X., Cornelis, R., Mees, L., Vanholder, R. and Lameire, N., *Analyst*, 1998, **123**, 13.
41 Costa-Fernández, J., Lunzer, F., Pereiro-Garcia, R., Sanz-Medel, A., and Bordel-Garcia, N., *J. Anal. At. Spectrom.*, 1995, **10**, 1019.
42 Hanna, C. P., Tyson, J. F., and McIntosh, S., *Clin. Chem.*, 1993, **39**, 1662.
43 Heitkemper, D., Creed, J., Caruso, J., and Fricke, F. L., *J. Anal. At. Spectrom.*, 1989, **4**, 279.
44 Larsen, E. H., Pritzl, G., and Hansen, S. H., *J. Anal. At. Spectrom.*, 1993, **8**, 557.
45 Feldmann, J., *Anal. Commun.*, 1996, **33**, 11.
46 Bavazzano, P., Perico, A., Rosendahl, K., and Apostoli, P., *J. Anal. At. Spectrom.*, 1996, **11**, 521.
47 Pergantis, S. A., Winnik, W., and Betowski, D., *J. Anal. At. Spectrom.*, 1997, **12**, 531.
48 Tsalev, D. L., Sperling, M., and Welz, B., to be published.
49 Lum, K., Naranjit, D., Radziuk, B., and Thomassen, Y., *Anal. Chim. Acta*, 1983, **155**, 183.
50 Crecelius, E., and Yager, J., *Environ. Health Perspect.*, 1997, **105**, 650.
51 Völlkopf, U., and Barnes, K., *At. Spectrosc.*, 1995, **16**, 19.
52 Nixon, D. E., and Moyer, T. P., *Spectrochim. Acta, Part B*, 1996, **51**, 13.

Paper 8/03044H
Received April 23, 1998
Accepted June 8, 1998